Blind Digital Tuning for Interference Cancellation in Full-Duplex Radio

Yingbo Hua, Yifan Li, Chaitanya Mauskar, and Qiping Zhu
Department of Electrical and Computer Engineering
University of California, Riverside, CA, 92521
yhua@ece.ucr.edu

***Abstract*—To make full-duplex radios, the most fundamental challenge known today is self-interference cancellation. This paper takes a new look at digitally controlled all-analog interference cancellation channel consisting of clustered taps (c-taps) of step-attenuators and other passive components such as RF power combiners and dividers. The performance of such a cancellation channel is robust to carrier frequency and attenuation-dependent phases of attenuators. Without the cost for and the errors from down-converting the input RF waveforms of any of the attenuators, a blind digital tuning algorithm based on the residual interference waveforms collected during a training phase is shown to be promising.**

I. Introduction

Interference cancellation is the most fundamental problem in realizing a full-duplex radio. For more than a century since radio communication was first invented, the world has not yet seen a commercially viable full-duplex radio that can transmit and receive at the same time and the same frequency. To our knowledge, the problem of self-interference in full-duplex radio is largely unsolved especially for high power and broadband applications.

Inside a full-duplex radio, there must be a transmit (Tx) chain and a receive (Rx) chain. The Tx chain converts a signal from baseband to radio frequency. The Rx chain converts a signal from radio frequency to baseband. Compared to the Rx chain, the Tx chain tends to be much noisier and nonlinear. To avoid the limitations of the Tx chain, an interference cancellation channel should typically tap the source of interference from the output of the Tx chain power amplifier [5] and [7] (not from the baseband of the Tx chain except for high quality transmitters on which transmit beamforming is based upon [6]). Furthermore, to avoid a potential saturation of the Rx chain by a high power interference, it is desired to cancel the interference before it reaches the low-noise-amplifier of the Rx chain. It is important to note that an interference is considered high power as long as it is much stronger than a desired signal to be received. A combination of the above two features leads to a strategy called all-analog cancellation in [7] and [9], which has also been previously attempted in [1], [3] and [4].

The MIT work shown in [1] assumes the complete knowledge of all the waveforms that are scaled by complex weights in an analog transversal filter. In practice, these waveforms are not only expensive to obtain by using additional down-converters but also inaccurate due to noise and biases from these down-converters. Also each of the complex weights is not easy to implement by using a variable attenuator and a variable phase. A practical attenuator has an attenuation-dependent phase and a practical phase adjuster has a phase-dependent insertion loss. The approach shown in [1] only yielded a 30dB 30MHz-bandwidth cancellation in a hardware-based test [2].

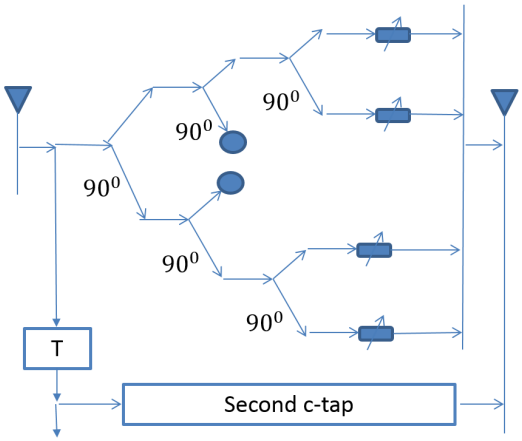

Fig. 1. An architecture of all-analog interference cancellation channel which follows the same idea conveyed by Fig. 8 in [9]. Each c-tap (clustered-tap of attenuators) has four branches evenly distributed in phase (not necessarily exactly). Each c-tap uses four variable/step attenuators. The branching-in arrows denote power combiners. The branching-out arrows denote power splitters. The heavy dots denote impedance-matching terminators. The in-air interference channel between the two antennas could be replaced by any isolation channel such as that in a circulator.

The Stanford work shown in [3] reports a prototype of full-duplex radio using a cancellation channel consisting of uniformly time-delayed attenuators. While impressive experimental data are reported there, it is known that the performance of such a cancellation channel is very sensitive to the carrier frequency as shown in [8]. A new architecture of the cancellation channel shown in [8] and [9] consists of multiple clustered-taps (c-taps) of attenuators. It can cancel $70dB$ $100MHz$-bandwidth interference with just 8 attenuators (two c-taps) for an interference channel with 1000 random multipaths of delay spread $1\mu s$. The performance of the new architecture is also robust to the carrier frequency as shown in [8]. More on this architecture will be discussed later.

The Intel work shown in [4] introduces a cancellation channel that has multiple time-delayed taps and each tap has multiple attenuators shifted with different phases. While independently developed, the cancellation channel architectures shown in [4] and [9] share a common feature in terms of a fixed phase-shifter connected to each attenuator. However, the

tuning algorithm developed in [4] relies on the measurement of the input signals to all attenuators, which is similar to that in [3]. The tuning algorithm developed in [9] does not require the input signal to any of the attenuators in the cancellation channel and hence saves a substantial hardware cost. This type of tuning algorithms is called blind digital tuning, which will be further discussed later.

This paper focuses on all-analog cancellation. Since all-analog cancellation using passive components virtually does not generate additional noise in the residual interference (in comparison to methods using active components), the hybrid and/or all-digital methods such as those discussed in [7] and [5] can be used as a following stage of interference cancellation in a practical full-duplex radio. The amount of interference cancellation referred to in this paper does not include the initial interference attenuation between a Tx antenna and a Rx antenna or via the isolation channel inside an RF circulator.

In section II, we revisit an all-analog cancellation channel previously shown in [8] and [9] and consider the effect of the attenuation-dependent phases of the attenuators. Also shown is a prototype of a c-tap of the all-analog cancellation channel. In section III, we revisit the approach of blind digital tuning previously shown in [9] and present a new algorithm. The statistical performance of the algorithm based on random realizations of the interference channel and the IQ imbalances in Tx and Rx chains is given in section IV.

II. Architecture of All-Analog Cancellation Channel

The architecture of the all-analog cancellation channel is crucial for ultimate performance of cancellation. A good architecture should have the following features: 1) it has a high capacity to match an interference channel affected by wireless scatterers around the Tx and/or Rx antennas; 2) it only uses reliable tunable devices; 3) it is highly integrable with the entire radio system.

The impulse response of a typical RF interference channel can be written as (subject to a frequency band of interest, e.g., $|f - fc| < 20MHz$):

$$h_{int,RF}(t) = \sum_{i=0}^{I-1} a_i \delta(t - \tau_i - T_0) \tag{1}$$

where I is the number of multipaths, a_i is the attenuation of the ith path, and $\tau_i + T_0$ is the delay of the ith path. Let the carrier frequency be f_c and the bandwidth of interest be W. Then, the baseband equivalent of $h_{int,RF}(t)$ is

$$h_{int}(t) = e^{-j2\pi f_c T_0} \sum_{i=0}^{I-1} a_i e^{-j2\pi f_c \tau_i} sinc(W(t - \tau_i - T_0)). \tag{2}$$

As the environment changes, the values of I, a_i and τ_i also change in general although T_0 can be pre-calibrated for a given setup of the Tx and Rx antennas. To be able to cancel the interference, the impulse response of the cancellation channel should be as close to the above equation as possible.

An architecture of the cancellation channel is shown in Fig. 1 where the only tunable devices are step attenuators. The technology of step-attenuators is rather mature. The difference between Fig. 1 and Fig. 8 in [9] is that here we have added additional 90-degrees power splitters to balance the insertion losses and phase shifts of all four branches in each tap (or c-tap). In this way, the (fixed) phase distribution among the four branches is about even and so is the insertion loss.

The impulse response of this cancellation channel is (subject to a frequency band of interest):

$$\begin{aligned} h_{can,RF}(t) &= \sum_{l=0}^{N-1} [P_0^3 g_{l,0} + P_0^2 P_{\pi/2} g_{l,1} + P_0 P_{\pi/2}^2 g_{l,2} \\ &\quad + P_{\pi/2}^3 g_{l,3}] \delta(t - lT - \hat{T}_0) \end{aligned} \tag{3}$$

where $g_{l,m}$ is the gain of the mth attenuator in the lth c-tap, P_0 is the transfer function for the 0-degree output of a 90-degree power splitter, and $P_{\pi/2}$ is the transfer function for the 90-degree output of the 90-degree power splitter. And $\hat{T}_0$ is an initial delay matched to T_0 of the interference channel, and T is the time delay between two adjacent c-taps. The baseband equivalent of $h_{can,RF}(t)$ is

$$h_{can}(t) = e^{-j2\pi f_c \hat{T}_0} \sum_{l=0}^{N-1} P_0^3 G_l e^{-j2\pi f_c lT} sinc(W(t - lT - \hat{T}_0)) \tag{4}$$

where $G_l = g_{l,0} - jg_{1,1} - g_{l,2} + jg_{l,3}$. Note that because of very large f_c (i.e., $f_c \gg W$), $[2\pi f_c \hat{T}_0]_{modulo-2\pi} \neq [2\pi f_c T_0]_{modulo-2\pi}$ while we can write $sinc(W(t - \hat{T}_0)) = sinc(W(t - T_0))$ with $|T_0 - \hat{T}_0| \ll \frac{1}{W}$ in practice. Also note that as long as $\hat{T}_0$ and P_0 are fixed, any imperfection in these values can be absorbed into the variables G_l and consequently into the variables $g_{l,m}$. What is important here is whether or not $h_{can}(t)$ (or its Fourier transform $H_{can}(f)$) can well match $h_{int}(t)$ (or its Fourier transform $H_{int}(f)$) once $g_{l,m}$ are optimized.

If $\max_{i \neq j} |\tau_i - \tau_j| \ll \frac{1}{W}$, it is easy to verify that even for $N = 1$ there exists a complex G_0 such that $h_{can}(t) = h_{int}(t)$. Otherwise, it is necessary to choose $N > 1$ for improved matching between $h_{can}(t)$ and $h_{int}(t)$.

The choice of T is important. From the classic sampling theory, it is known that since $h_{int}(t)$ has the (double-sided) bandwidth W, there exist $\hat{G}_l$ for $-\infty < l < \infty$ such that $\sum_{l=-\infty}^{\infty} \hat{G}_l sinc(W(t - lT - T_0))$ with $T = \frac{1}{W}$ can match $h_{int}(t)$ exactly. But a problem with this sampling theory is that if $T = \frac{1}{W}$ then the number of required c-taps N can be very large even when the delay spread $\max_{i \neq j} |\tau_i - \tau_j|$ is in the order of $\frac{1}{W}$. Such a delay spread is typical for a full-duplex radio with $W = 20 \sim 40MHz$. To reduce the number of the c-taps, we suggest to choose T as a small fraction of $\frac{1}{W}$. Intuitively, in this way, each c-tap is effectively used to model a cluster of multipaths with a delay spread equal to that fraction of $\frac{1}{W}$. The definition of bandwidth W varies according to application. Since we are interested in interference cancellation all the way to the receiver noise floor, the bandwidth W referred to earlier should be the bandwidth of interest at the noise floor. This could be larger than a 40dB-drop (for example) bandwidth of a high power interference.

There is a fundamental difference between Fig. 1 and that in Fig. 3 in [3]. In the latter, fixed delays are evenly distributed among all attenuators. As shown in [8], such an architecture

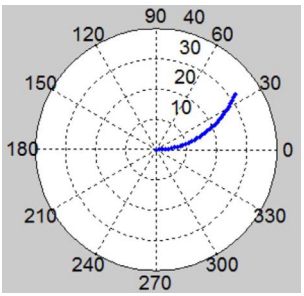

(a) 1 attenuator per c-tap. $G = g_0$.

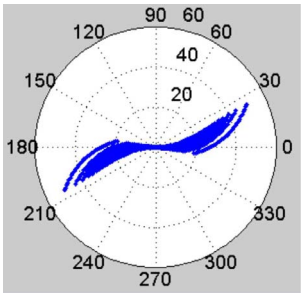

(b) 2 attenuators per c-tap. $G = g_0 - g_1$.

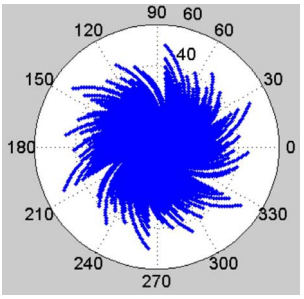

(c) 3 attenuator per c-tap. $G = g_0 + e^{-j2\pi/3}g_1 + e^{j2\pi/3}g_2$.

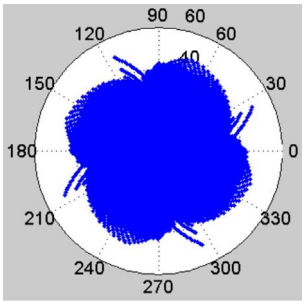

(d) 4 attenuators per c-tap. $G = g_0 - jg_1 - g_2 + jg_3$.

Fig. 2. Impedance coverage of a single c-tap where each attenuator (i.e., g_i, $i = 0, 1, 2, 3$) has the attenuation range (i.e., range of $-20\log_{10}|g_i|$) from 0dB to 32dB with 1dB step size. Each attenuator also has an attenuation-dependent phase (i.e., $\arg(g_i) = -\alpha 20\log_{10}|g_i|$ with $\alpha = 1.1$). Each of the plots shows the coverage of $(-20\log_{10}|G|)e^{j\arg(G)}$.

with uniformly distributed attenuators with respect to delays can suffer serious performance degradation depending on the choice of carrier frequency. In particular, if the time delay between two adjacent attenuators is $T_u = \frac{m}{f_c}$ with m being an integer, then the cancellation channel loses all its capacity to match the interference channel. The heuristic justifications given in [3] (see the 1st column of page 4 there) missed an important fact that the RF interference channel is a bandpass channel. If the authors of [3] actually referred to the highest frequency of the RF interference in their application of the sampling theory, then the required delay between samples would be no larger $0.23ps$ for $f_c = 2.2GHz$. Then for a multipath delay spread of $10ns$ (corresponding to just $3m$ distance difference), they would need at least 43×10^3 delay lines and the same number of attenuators.

Unlike that in [3], the architecture shown in Fig. 1 is robust to carrier frequencies. The capacity of how well this architecture can match an interference channel with 1000 random multipaths and a delay spread of $1\mu s$ is studied in [8] and [9]. With just two or more taps and $T = \frac{0.1}{W}$, the architecture in Fig. 1 can cancel $70 \sim 80dB$ $100MHz$-bandwidth interference.

To demonstrate that using four attenuators evenly distributed in phase per tap is a good choice, let us look at the per-tap impedance coverage shown in Fig. 2 for each of the four cases: i.e., one, two, three or four attenuators evenly distributed in phase per tap. It is clear that the coverage shown in Fig. 2(d) is the most desirable since its coverage is the most dense.

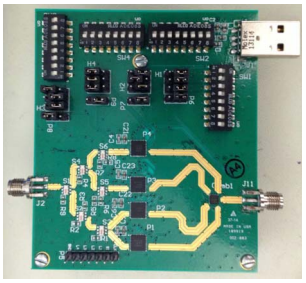

(a) Custom fabricated PCB of a single c-tap.

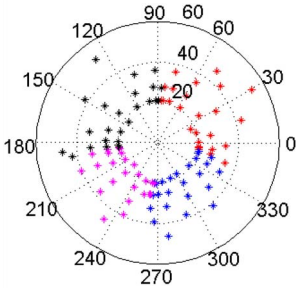

(b) 100 (out of 32^4) measured samples of impedance of the c-tap.

Fig. 3. A prototype of c-tap using four step-attenuators (PE43703), six (could be five) 90-degree splitters (QCN27) and a power combiner (WP4U1+).

A custom fabricated single c-tap PCB, based on a slight variation of Fig. 1, is shown in Fig. 3(a). One hundred (out of 32^4) samples of the effective impedance of the implemented single c-tap is shown in Fig. 3(b). The red group samples, for example, were collected when each of the 1st and 2nd attenuators was set at 1dB, 7dB, 14dB, 21dB and 28dB (total 25 combinations), and 3rd and 4th attenuators were both set at 31.75dB. The data from this prototype confirm the desired property of the c-tap.

III. Blind Digital Tuning

While an all-analog cancellation channel such as Fig. 1 has a high capacity to match an interference channel of random multipaths over a wide bandwidth (and it is also robust to the choice of carrier frequency), online tuning of the cancellation channel is a separate challenge. Online tuning is necessary since the interference channel is affected by wireless scatterers in the environment around the Tx and Rx antennas. As reported in [3], for every $100ms$, the cancellation channel of a WiFi in full-duplex mode would need to be re-tuned. For hand-held devices, the required tuning would be more frequent.

A classic approach for online tuning of the cancellation channel is as follows:

$$\min_{g_{l,i}\forall l,i} E\left\|y(t) - \sum_{l=0}^{N-1}\sum_{i=0}^{P-1} g_{l,i}x_{l,i}(t)\right\|^2 \quad (5)$$

where $P = 4$ for Fig. 1, $y(t)$ is the interference before cancellation, and $x_{l,i}(t)$ are the input signals to the attenuators. Measuring $x_{l,i}(t)$ requires special hardware, which is very costly especially when $N > 1$. Cheap hardware would not measure $x_{l,i}(t)$ accurately. The tuning method shown in [4] follows this classic approach. They applied the LMS (least-mean-square) algorithm and observed a rather poor convergence property when the down-converters used for measuring $x_{l,i}(t)\forall l, i$ have a small amount of IQ imbalances and phase noise. These impairments are only part of the reality. Due to analog interfaces of the RF attenuators in the circuits, the input waveforms $x_{l,i}(t)\forall l, i$ to the attenuators are *inherently ambiguous* along with the actual attenuations of the attenuators. Every analog connector introduces an unknown insertion loss and phase.

To avoid the cost and the errors in measuring $x_{l,i}(t)\forall l, i$, there is a new approach called blind digital tuning. This

approach was first presented in [7] and then refined in [9]. Blind digital tuning has two basic phases. In phase 1, a training process is conducted to learn the relationship between the *controllable values* of attenuations of the attenuators and the *observable values* of the residual interference. In phase 2, a computational optimization process is executed to determine the *optimal controllable values* of the attenuators. The controllable value of the attenuation of an attenuator does not need to be the same as the actual attenuation that an attenuator brings to the circuit. The mismatch between the controllable values and the actual values is absorbed into the system model established in the training phase. The controllable values are typically *digitally controllable*. Blind digital tuning is blind to the input waveforms of the attenuators.

In [9], the observable value of the residual interference is assumed to be the power of the residual interference. Assuming a linearity between the controllable gains (inverses of attenuations) of the attenuators and the residual interference waveform, the power of the residual interference is a quadratic function of the controllable attenuations:

$$e_p = \mathbf{g}^T \mathbf{A} \mathbf{g} + \mathbf{b}^T \mathbf{g} + c \tag{6}$$

where e_p denotes the averaged power of the residual interference, $\mathbf{g}$ is a real-valued vector of the controllable gain values. And the real matrix $\mathbf{A}$, the real vector $\mathbf{b}$ and the real number c are all unknowns and need to be estimated during training. Measuring the residual interference typically requires a down-converter which almost always has some level of IQ imbalances. Using real-valued data representation, the IQ imbalances do not destroy the linearity [9]. The linearity between the gain of an attenuator and its output typically holds strongly. To estimate $\mathbf{A}$, $\mathbf{b}$ and c, a sequence of training vectors of $\mathbf{g}$ has been developed in [9].

In this paper, we assume that the observable values of the residual interference are the entire waveforms of the residual interference. Let $e(t)$ be the observed waveform of residual interference in the baseband in response to a training vector $\mathbf{g}$. Here, $\mathbf{g} = [\mathbf{g}_0^T, \cdots, \mathbf{g}_{N-1}^T]^T$ with $\mathbf{g}_l = [Re\{g_{l,0}\}, Im\{g_{l,0}\}, \cdots, Re\{g_{l,3}\}, Im\{g_{l,3}\}]^T$. Let $\mathbf{e} = [Re\{e(0)\}, Im\{e(0)\}, \cdots, Re\{e((K-1)T_s)\}, Im\{e((K-1)T_s)\}]^T$ with K being the number of samples and T_s being the sampling interval. Here, we can choose $T_s = \frac{1}{W}$. It follows that

$$\mathbf{e} = \mathbf{y} - \mathbf{X}\mathbf{g} + \mathbf{v} = \bar{\mathbf{X}}\bar{\mathbf{g}} + \mathbf{v} \tag{7}$$

where $\mathbf{v}$ is the receiver noise, $\bar{\mathbf{X}} = [\mathbf{y}, \mathbf{X}] \in R^{2K \times (8N+1)}$ and $\bar{\mathbf{g}} = [1, -\mathbf{g}^T]^T \in R^{(8N+1)\times 1}$. And both $\mathbf{y}$ and $\mathbf{X}$ are treated as unknowns although $\mathbf{y}$ corresponds to the interference before cancellation. During training, the transmitted power and/or the sensitivity of the receiver can be reduced to avoid saturation.

Assume a sequence of training vectors of $\bar{\mathbf{g}}$, i.e., $\bar{\mathbf{g}}^{(0)}, \cdots, \bar{\mathbf{g}}^{(N_g-1)}$. For the ith training vector $\bar{\mathbf{g}}^{(i)}$, we can measure the corresponding $\mathbf{e}$ for N_t times to obtain: $\mathbf{e}^{(i,0)}, \cdots, \mathbf{e}^{(i,N_t-1)}$. It follows that $\mathbf{e}^{(i,r)} = \bar{\mathbf{X}}^{(i,r)}\bar{\mathbf{g}}^{(i)} + \mathbf{v}^{(i,r)}$ where $\bar{\mathbf{X}}^{(i,r)}$ is subject to Tx random noise. We then compute $\mathbf{e}^{(i)} = \frac{1}{N_t}\sum_{r=0}^{N_t-1}\mathbf{e}^{(i,r)}$, and therefore for either large N_t or low receive noise, $\mathbf{e}^{(i)} = \bar{\mathbf{X}}^{(i)}\mathbf{g}^{(i)}$ where $\bar{\mathbf{X}}^{(i)} = \frac{1}{N_t}\sum_{r=0}^{N_t-1}\bar{\mathbf{X}}^{(i,r)}$. Also, for either large N_t or low transmit noise, $\bar{\mathbf{X}}^{(i)}$ should be invariant to i. For this reason, we can now write $\mathbf{e}^{(i)} = \bar{\mathbf{X}}\mathbf{g}^{(i)}$.

Let $\mathbf{E} = [\mathbf{e}^{(0)}, \cdots, \mathbf{e}^{(N_g-1)}]$ and $\bar{\mathbf{G}} = [\bar{\mathbf{g}}^{(0)}, \cdots, \bar{\mathbf{g}}^{(N_g-1)}]$. It follows that

$$\mathbf{E} = \bar{\mathbf{X}}\bar{\mathbf{G}} \tag{8}$$

If $\bar{\mathbf{G}}$ has a full row rank, then the least square solution to the above equation is

$$\bar{\mathbf{X}} = \mathbf{E}\bar{\mathbf{G}}^+ = \mathbf{E}\bar{\mathbf{G}}^T(\bar{\mathbf{G}}\bar{\mathbf{G}}^T)^{-1} \tag{9}$$

From $\bar{\mathbf{X}}$, we then obtain $\mathbf{y}$ and $\mathbf{X}$. The optimal $\mathbf{g}$ is given by

$$\mathbf{g} = \mathbf{X}^+\mathbf{y} = (\mathbf{X}^T\mathbf{X})^{-1}\mathbf{X}^T\mathbf{y} \tag{10}$$

There are numerous choices for $\bar{\mathbf{G}}$ with a full row rank. To show such an example, let us assume $N = 1$. Then, we can choose $N_g = 0$ and

$$\bar{\mathbf{G}} = \begin{bmatrix} 1 & 1 & 1 & 1 & 1 & 1 & 1 & 1 & 1 \\ 0 & 1 & 0 & 0 & 0 & 0.15 & 0 & 0 & 0 \\ 0 & 0 & 0 & 0 & 0 & 0.5 & 0 & 0 & 0 \\ 0 & 0 & 1 & 0 & 0 & 0 & 0.15 & 0 & 0 \\ 0 & 0 & 0 & 0 & 0 & 0 & 0.5 & 0 & 0 \\ 0 & 0 & 0 & 1 & 0 & 0 & 0 & 0.15 & 0 \\ 0 & 0 & 0 & 0 & 0 & 0 & 0 & 0.5 & 0 \\ 0 & 0 & 0 & 0 & 1 & 0 & 0 & 0 & 0.15 \\ 0 & 0 & 0 & 0 & 0 & 0 & 0 & 0 & 0.5 \end{bmatrix} \tag{11}$$

where each entry $\bar{\mathbf{G}}$ except the first row is a real or imaginary component of a complex gain, e.g., 1 corresponds to $0dB$ attenuation, 0 to maximum attenuation (32dB in simulation), and the number $0.15 + j0.5$ to 16dB attenuation along with an attenuation-dependent phase. The example of $\bar{\mathbf{G}}$ shown above is a good one because of its sparseness useful for computation.

While the phase constraint on the attenuators (the attenuation-dependent phase) is easy to impose in choosing $\bar{\mathbf{G}}$, the solution from (10) does not automatically meet the phase constraint. One way to solve this problem is to use the following equation for each c-tap (lth c-tap):

$$g_{l,0} - jg_{l,1} - g_{l,2} + jg_{l,3} = \hat{g}_{l,0} - j\hat{g}_{l,1} - \hat{g}_{l,2} + j\hat{g}_{l,3} \tag{12}$$

where the left-hand-side terms are chosen from (10) and the right-hand-side terms meet the phase constraint. In particular, when step-attenuators are used, we can use a brute-force search for the best choice of the right-hand-side terms. The complexity is in the order of $\left(\frac{D_{dB}}{d_{dB}}\right)^4 N$ where D_{dB} is the dynamic range in dB of each step-attenuator and d_{dB} is the step size in dB. In practice, we can pre-calibrate each c-tap digitally. The digital map of the c-tap is readily useful for blind digital tuning.

IV. Simulation

The simulation follows Fig. 4. There are random Tx and Rx I/Q imbalances. The effect of Tx I/Q imbalances on the real and imaginary components of $x[n]$ is equivalent to multiplying $[Re\{x[n]\}, Im\{x[n]\}]^T$ by the matrix:

$$\begin{bmatrix} (1+\delta_T)\cos\theta_T & (1-\delta_T)\sin\theta_T \\ (1+\delta_T)\sin\theta_T & (1-\delta_T)\cos\theta_T \end{bmatrix} \tag{13}$$

For the Rx I/Q imbalances, the matrix is

$$\begin{bmatrix} (1+\delta_R)\cos\theta_R & (1+\delta_R)\sin\theta_R \\ (1-\delta_R)\sin\theta_R & (1-\delta_R)\cos\theta_R \end{bmatrix} \tag{14}$$

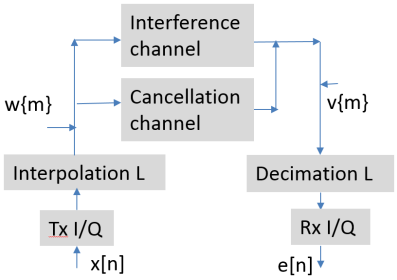

Fig. 4. System diagram for simulation. The analog components are represented by those operating at a frequency L-times higher than the baseband frequency.

The parameters δ_T, θ_T, δ_R and θ_R are uniformly random between $[-0.05, 0.05]$. The sampling rate for the baseband waveform $x[n]$ equals $W = 40MHz$. The components after the interpolator and before the decimator are operating at the sampling rate equal to LW where $L = 500$. $w\{m\}$ and $v\{m\}$ are the Tx and Rx noises. The corresponding signal-to-noise ratios are denoted by SNR_T and SNR_R. The responses of the interference and cancellation channels are represented by $h_{int}(\frac{m}{LW})$ and $h_{can}(\frac{m}{LW})$ respectively from (2) and (4).

The attenuation factors of the multipaths in (2) have the form

$$a_i = \frac{\epsilon\alpha_i}{(d + c\tau_i)^2} \tag{15}$$

where $a_0 = \frac{\epsilon}{d^2}$, $c = 3 \times 10^8$m/s, $d = 0.3$m, $0 \le \tau_i \le 10$ns (uniform random), $0 \le \alpha_i \le 1$ (uniform random) and $\epsilon = 8 \times 10^{-4}$. Also, $I = 100$.

Shown in Fig. 5 are the cumulative distribution functions (CDF) of the normalized power of residual interference after the cancellation optimized by blind digital tuning. The normalized power equals $0dB$ before any cancellation. There are four cases shown here. For Fig. 5(a), there are no Tx/Rx noise and no quantization of attenuators. For Fig. 5(b), there are Tx/Rx noise such that $SNR_T = 30dB$ and $SNR_R = 60dB$ but no quantization of attenuators. For Fig. 5(c), there are the same noise and $0.5dB$ step size for attenuators. For Fig. 5(d), there are the same noise and $1dB$ step size for attenuators. Note that the "signal" used in computing SNR_T is everything at the output of the Tx chain except $w\{m\}$, and the "signal" used on computing SNR_R is everything at the RF frontend of the Rx chain except $v\{m\}$. We see that the step size of the attenuators has a major impact on the performances. Due to space limitation, we omit the results for smaller step sizes such as $0.25dB$ which is also common in practice. Also omitted are results of the improvement of two-stage cancellation over single-stage cancellation.

V. Conclusion

In this paper, we have revisited an all-analog interference cancellation channel using c-taps of digitally controllable attenuators and a blind digital tuning approach. The presented architecture of all-analog cancellation channel has a very high capacity to match a randomly given interference channel. The blind digital tuning algorithm shown in this paper can realize the capacity of the all-analog cancellation channel without the cost of and the errors from down-converting the input RF waveforms of any of the step-attenuators in the cancellation channel.

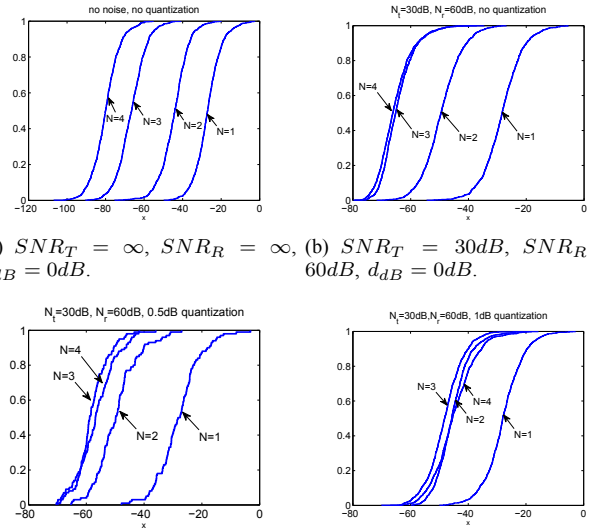

(a) $SNR_T = \infty$, $SNR_R = \infty$, $d_{dB} = 0dB$. (b) $SNR_T = 30dB$, $SNR_R = 60dB$, $d_{dB} = 0dB$.

(c) $SNR_T = 30dB$, $SNR_R = 60dB$, $d_{dB} = 0.5dB$. (d) $SNR_T = 30dB$, $SNR_R = 60dB$, $d_{dB} = 1dB$.

Fig. 5. CDF of normalized powers in dB of residual interferences after optimized cancellations.

Acknowledgment

This work was supported in part by ARO under Contract No. W911NF1210432 and UCOP under Grant No. PC-12-247260.

References

[1] J. G. McMichael and K. E. Kolodziej, "Optimal Tuning of Analog Self-Interference Cancellers for Full-Duplex Wireless Communication," In *Proc. Allerton Conference*, 2012.

[2] K.E. Kolodziej, J.G. McMichael, B.T. Perry, "Adaptive RF Canceller for Transmit-Receive Isolation Improvement," *Radio and Wireless Symposium*, Newport Beach, CA, 2014

[3] D. Bharadia, E. McMilin, and S. Katti, "Full Duplex Radios", *Sigcomm* 2013.

[4] Y.-S. Choi and H. Shirani-Mehr, "Simultaneous Transmission and Reception: Algorithm, Design and System Level Performance", *IEEE Transactions on Wireless Communications*, 2013, to appear (posted at Arxiv).

[5] S. H. Li and R. D. Murch, "Full-Duplex Wireless Communication Using Transmitter Output Based Echo Cancellation," in *Proc. 2011 IEEE Global Commun. Conf.*, pp. 1-5.

[6] Y. Hua, P. Liang, Y. Ma, A. Cirik and Q. Gao, "A method for broadband full-duplex radio", *IEEE Signal Processing Letters*, Vol. 19, No. 12, pp. 793-796, Dec 2012.

[7] Y. Hua, Y. Ma, P. Liang and A. Cirik, "Breaking the Barrier of Transmission Noise in Full-Duplex Radio," *MILCOM 2013*, San Diego, CA, Nov 2013.

[8] A. Gholian, Y. Ma and Y. Hua, "A Numerical Investigation of All-Analog Radio Self-Interference Cancellation," *IEEE Workshop on SPAWC*, Toronto, Canada, June 2014.

[9] Y. Hua, Y. Ma, A. Gholian, Y. Li, A. Cirik and P. Liang, "Radio Self-Interference Cancellation by Transmit Beamforming, All-Analog Cancellation and Blind Digital Tuning," *Signal Processing*, Volume 108, March 2015, Pages 322-340. DOI: 10.1016/j.sigpro.2014.09.025.